DETERMINATION OF VS30 FOR SEISMIC GROUND CLASSIFICATION IN THE LJUBLJANA AREA, SLOVENIA

JANEZ ROŠER and ANDREJ GOSAR

About the authors

Janez Rošer
University of Ljubljana,
Faculty of Natural Sciences and Engineering
Aškerčeva 12, 1000 Ljubljana, Slovenia
E-mail: janez.roser@ntf.uni-lj.si

Andrej Gosar
University of Ljubljana,
Faculty of Natural Sciences and Engineering
and Environmental Agency of Slovenia,
Seismology and Geology Office
Dunajska 47, 1000 Ljubljana, Slovenia
E-mail: andrej.gosar@gov.si

Abstract

Ljubljana, the capital of Slovenia, is located in the central region of the country in a shallow sedimentary basin filled with Quaternary deposits. It is one of the most seismically active regions in Slovenia, with some important historical earthquakes that have caused damage and economic losses. The soft sediments are some of the most important factors responsible for the amplification of seismic ground motions in the area. The existing microzonation studies in the Ljubljana basin are inadequate, since there is a lack of borehole and geophysical data. Thus, investigations of the seismic shear-wave velocity for the purposes of supplementing the existing seismic microzonation of Ljubljana were carried out. The average shear-wave velocity for the topmost 30 m of sediments at 30 sites was determined using the joint modelling of three-component, microtremor, horizontal-to-vertical spectral ratio (HVSR) data and dispersion curves obtained through microtremor array measurements analyzed by the Extended Spatial Autocorrelation (ESAC) and Refraction Microtremor (ReMi) methods. The phase-velocity dispersion curves obtained from the ESAC and ReMi analysis of the microtremor record showed very good agreement. The estimated Vs30 values are higher in the northern and north-eastern parts of the study area (300–600 m/s), where the Pleistocene and Holocene glaciofluvial deposits of the Sava River, mostly gravel and sand, are dominant. In the southern part of the city (140–300 m/s) the lowest values of Vs30 correspond to the lacustrine and fluvial deposits of the Ljubljana Moor. The results are in good agreement with the distribution of the sedimentary units, while in comparison with the existing EC8 based microzonation, the investigated area can be classified, generally, as being one class better in terms of the EC8 classification. The obtained spatial distribution of Vs30 in Ljubljana therefore provides valuable information to supplement the existing microzonation.

Keywords

microtremor survey methods, shear-wave velocity, seismic site effects, microzonation, Eurocode 8

1 INTRODUCTION

The extended area of Ljubljana, the capital of Slovenia, is the most densely populated area in the country, with more than 300,000 inhabitants. It is located in central Slovenia in a young, shallow, sedimentary basin filled with Quaternary deposits. The basin is located in one of the three areas with the highest level of seismic hazard in Slovenia. A number of earthquakes devastated Ljubljana (Figure 1), including the strongest historical earthquake in Slovenia, the Idrija earthquake of 1511, with its epicentre approximately 30 km west of Ljubljana, and the Ljubljana earthquake of 1895. The estimated magnitude of the Idrija earthquake was M = 6.8, and the maximum intensity in the Ljubljana region was VIII-IX MSK. The Ljubljana earthquake, which had a magnitude of M=6.1 and a maximum intensity VIII-IX MSK, caused a great deal of damage, more than 100 buildings were destroyed, although the number of casualties was small. The Litija earthquake in 1963 (M=4.9) had, in Ljubljana, an intensity VI-VII MSK.

Ground motion is controlled by a number of variables, including the characteristic of the source, the propagation path and the near-surface geology. Phenomena associated with the propagation of seismic waves through the subsurface are modified by several effects, as described in Anderson (2007). The amplification of

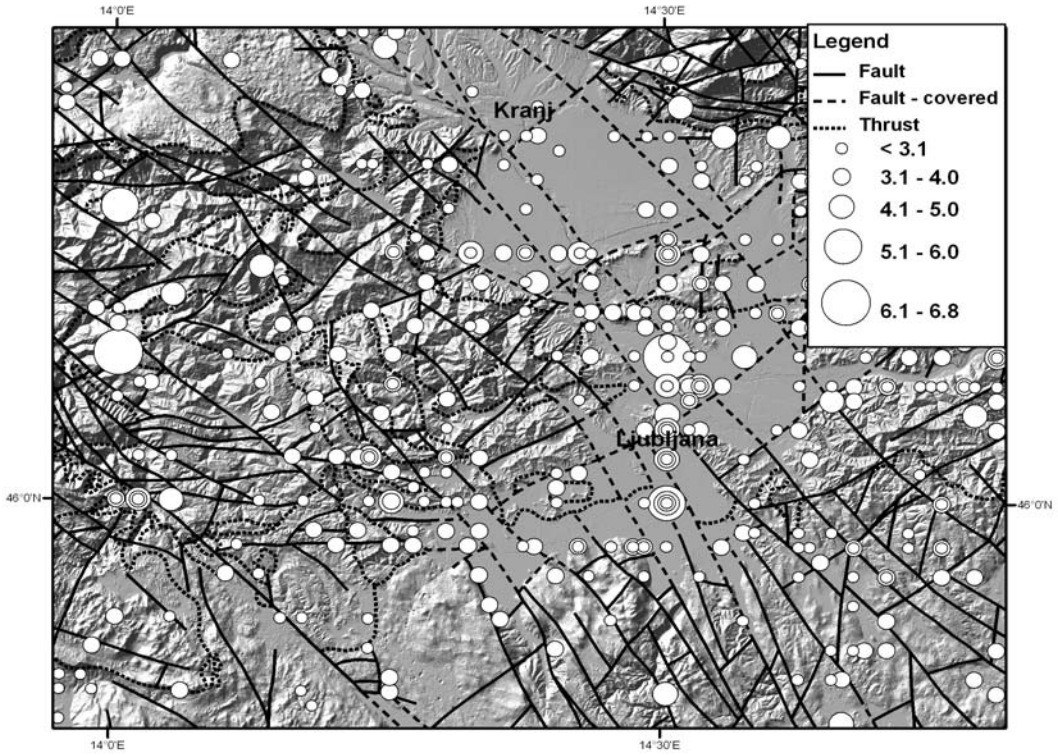

Figure 1. Seismicity of the extended Ljubljana region with generalized tectonic elements (after Grad and Ferjančič, 1974; Premru, 1982).

seismic waves is closely linked with areas where a strong acoustic impedance is present, i.e., where layers of low seismic velocity overlie stiff soils or bedrock with a high seismic velocity. The amplification A is proportional to the reciprocal square root of the product of the shear-wave velocity V_s and the density ρ of the investigated soil (Aki and Richards, 2002):

$$A \propto \frac{1}{\sqrt{V_s \, \rho}} \qquad (1)$$

where ρ is, in general, relatively constant with depth, and the V_s profile better describes the local site conditions. The most important parameter in the classification of the soil response is the average shear-wave velocity in the topmost 30 m of sediments, the *Vs30*. This quantity is also used in the building code Eurocode 8 (EC8) to classify sites according to soil type into five major categories, and two specific categories that correspond to very loose or liquefiable material (Table 1) (CEN, 2004 and SIST EN 1998-1, 2005). In the case that the value of *Vs30* is unknown, the value of N_{SPT} (the number of blows in a Standard Penetration Test) or c_u (the undrained shear strength) can be used. Although *Vs30* is used as a key parameter to classify soils, no consensus exists on its effectiveness as a proxy to site amplification (Castellaro et al., 2008).

The main task of microzonation is mapping the area prone to locally amplified ground motion (site effects). A suitable characterization of the local site effects can be performed by determining the resonance frequency of soft sedimentary layers (e.g., Gosar et al., 2010), or by estimating the local shear-wave velocity profiles.

In this work, in order to provide additional useful information for site effects and microzonation studies in the Ljubljana area, a series of 30 microtremor array measurements utilizing 4.5-Hz geophones and high dynamic digitizers were carried out at selected sites of the study area. The extended spatial autocorrelation method (ESAC) (Aki, 1957; Ohori et al., 2002; Okada, 2003) and the refraction microtremor method (ReMi) (Louie, 2001) were used to estimate the Rayleigh wave-dispersion curves and the wavefield analyses. In addition, three-component, single-station microtremor measurements were performed and analyzed using the

Table 1. Soil classification according to Eurocode 8 (CEN, 2004 and SIST EN 1998-1, 2005)

Ground type	Description of stratigraphic profile	Parameters		
		Vs30 (m/s) (shear-wave velocity)	N_{SPT} (standard penetration test) (blows/30cm)	c_u (kPa) (undrained shear strength)
A	Rock or other rock-like geological formation, including at most 5 m of weaker material at the surface.	> 800	–	–
B	Deposits of very dense sand, gravel, or very stiff clay, at least several tens of metres in thickness, characterised by a gradual increase of mechanical properties with depth.	360–800	> 50	> 250
C	Deep deposits of dense or medium-dense sand, gravel or stiff clay with thicknesses from several tens to many hundreds of metres.	180–360	15–50	70–250
D	Deposits of loose-to-medium cohesionless soil (with or without some soft cohesive layers), or of predominantly soft-to-firm cohesive soil.	< 180	< 15	< 70
E	A soil profile consisting of a surface alluvium layer with vs values of type C or D and thickness varying between about 5 m and 20 m, underlain by stiffer material with vs > 800 m/s.			
S1	Deposits consisting of, or containing, a layer at least 10 m thick, of soft clays/silts with a high plasticity index (PI > 40) and a high water content.	< 100 (indicative)	–	10–20
S2	Deposits of liquefiable soils, of sensitive clays, or any other soil profile not included in types A– E or S1.			

horizontal-to-vertical spectral ratio (HVSR) method. The dispersion curves obtained by the array measurements were used together with the HVSR curves in a joint modelling to estimate the shear-wave velocity profiles in the topmost 30 m of the sediments.

2 GEOLOGICAL SETTING

Ljubljana is situated in a young, shallow, sedimentary tectonic basin. In general, we distinguish two main parts: the Ljubljana Field in the north and the Ljubljana Moor in the south. The geological map of the surveyed area is shown in Figure 2. The bedrock of the basin is built partly of Carboniferous and Permian clastic rocks – dark-grey schistosuous claystones, mica and quartz siltstones, quartz sandstones and fine-grained conglomerates – and partly of Triassic and Jurassic limestone and dolomite (Žlebnik, 1971; Mencej, 1989). The bedrock outcrops in the hills surrounding the basin.

The Ljubljana Field is a tectonic depression that was formed in Pleistocene and has been filled with the Pleistocene and Holocene glaciofluvial deposits of the Sava River. These are composed mainly of carbonate gravel, interbedded with lenses or layers of conglomerate (Grad and Ferjančič, 1974; Premru, 1982). The total thickness of the sediments in the Ljubljana Field is very variable and in the central part exceeds 100 m.

The Ljubljana Moor basin is filled with unconsolidated lacustrine and fluvial Quaternary sediments composed of clay, gravel, sand, silt and chalk, which are up to 200 m thick. The uppermost layers are very soft. The basin is cut by several faults, striking in the NW-SE direction, while the faults striking in the NE-SW and E-W direction are less important. These faults separate the bedrock into different blocks. The differential subsidence of the tectonic blocks results in a pronounced bedrock topography.

Site effects due to the wave trapping inside soft sediments are characteristic of the whole city area, but they can be especially strong in the southern part.

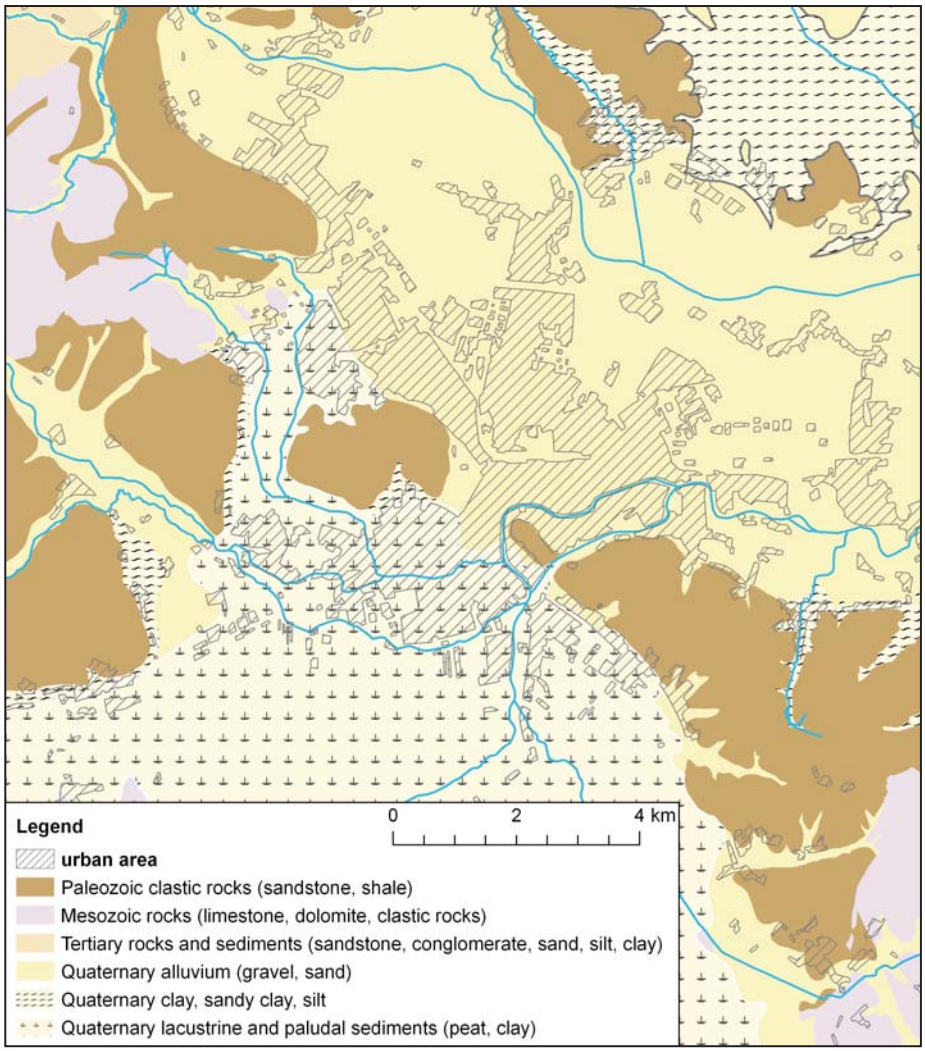

Figure 2. Simplified geological map of the Ljubljana region (after Grad and Ferjančič, 1974; Premru, 1982)

3 PREVIOUS MICROZONATION STUDIES

The importance of the city of Ljubljana and the past occurrence of large earthquakes have provoked several attempts at a microzonation of the city. The first one was carried out by Lapajne in 1970 (Lapajne, 1970). It was based on the nowadays outdated methodology of Medvedev (Medvedev, 1965), where intensity increments in the Medvedev-Sponheuer-Karnik (MSK) scale were calculated. The data used in this microzonation study were acquired from surface geology, geotechnical boreholes and seismic refraction measurements of the longitudinal wave velocities. Later on there were two studies, which did not involve any new field investigations: a microzonation made by Vidrih et al. (1991) and, after the publication of a new national probabilistic seismic hazard map for a 475-year return period (Lapajne et al., 2001), a microzonation based on the EC8 standard by Zupančič et al. (2004). The latter was based on the surface geological map and a rough estimate of the shear-wave velocities from existing longitudinal wave velocities. From this map the Municipality of Ljubljana can be roughly divided into three parts. The northern part of Ljubljana was classified as ground type C with a minor part as ground type D. The west part of Ljubljana is classified as ground type E and the southern part as ground type S1 (Figure 12). The main weakness of the described microzonations is the lack of in-situ, shear-wave velocity information, because only at three locations were the shear-wave refraction seismic data available.

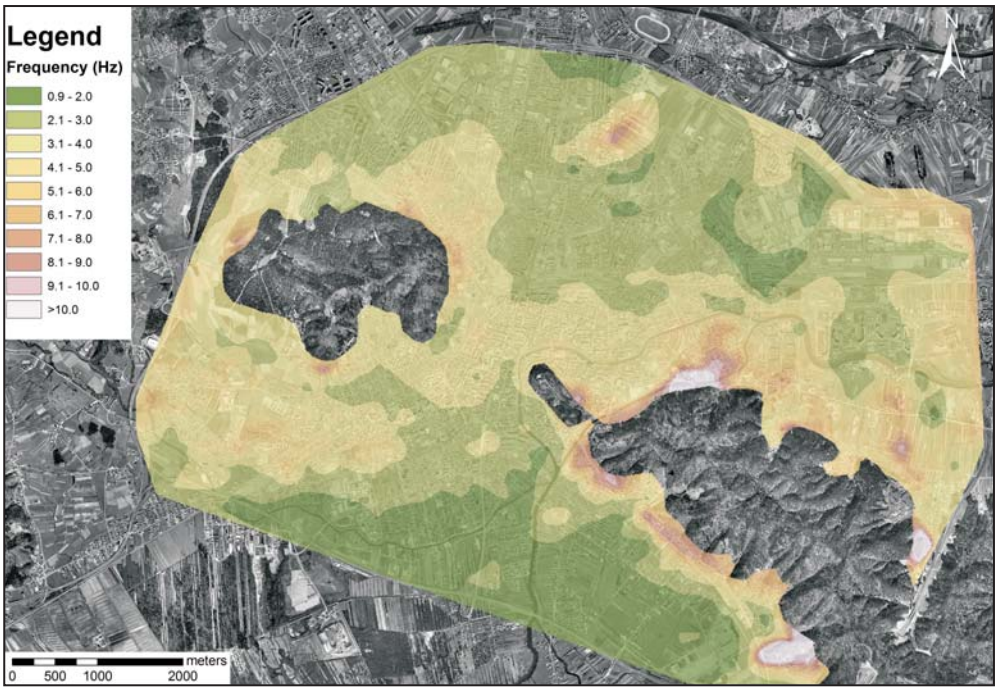

Figure 3. Map of the sediment resonance frequency derived from HVSR data (Gosar et al., 2010)

In 2009 a new quantitative microzonation of Ljubljana was made by Gosar et al. (2010). The microtremor horizontal-to-vertical spectral ratio method was applied to 1223 measuring points in an approximately 200 m × 200 m dense grid in order to assess the fundamental frequency of the soft sediments overlying bedrock. The iso-frequency map of sediments (Figure 3) shows a distribution in the range 0.9 to 10 Hz. The average frequency in the northern part is 3.5 ± 1.4 Hz, and in the southern part it is 2.9 ± 1.5 Hz (Gosar et al., 2010). However, this study did not provide any information about the shear-wave velocities in sediments.

Thus, we started with investigations of the seismic shear-wave velocity for the purposes of supplementing the existing seismic microzonations of Ljubljana.

4 METHODOLOGY

In this study we used three passive methods to analyse the microtremor records. The first one is based on three-component, single-station measurements and is called the horizontal-to-vertical spectral ratio (HVSR) method. The next two methods belong to the array measurements: the extended spatial autocorrelation method (ESAC) (e.g., Okada, 2003) and the refraction microtremor method (ReMi) (Louie, 2001). The basic principle of the array-survey methods is an analysis of the form of dispersion of the surface waves contained in the microtremors, i.e., determining the relationship between the phase velocity and the frequency (Okada, 2003). Common to all three methods is the assumption of horizontal soil layering under the observation area.

4.1 THE HORIZONTAL-TO-VERTICAL SPECTRAL RATIO (HVSR) METHOD

First applied by Nogoshi and Igarashi (1970 and 1971) and made well known by Nakamura (1989 and 2000), the use of the horizontal-to-vertical spectral ratio (HVSR) method to derive the fundamental frequency of soft sediments overlying bedrock has become increasingly popular because of its simplicity in terms of application and its low cost. The HVSR value at each frequency is defined as

$$HVSR(f) = \frac{\sqrt{H_{NS}(f) \cdot H_{EW}(f)}}{V(f)} \qquad (2)$$

where H and V denote the spectra of the horizontal (North-South and East-West direction) and vertical components, respectively. The frequency of the HVSR

peak reflects the fundamental frequency of the sediments. The basic assumption of the HVSR method is that the vertical component of the ground motion in cases where the soil stratigraphy is plane-parallel is supposed to be free of any kind of influence related to the soil conditions at the recording site. An overview of the method was presented by Bard (1999), and Mucciarelli and Gallipoli (2001).

Despite the fact that the theoretical basis is still debated there is a consensus that this ratio allows us to estimate, with reasonable accuracy, the principal shear-wave resonance frequency *f* of the sedimentary cover overlying infinite bedrock. For the simplest case of a single-layer, one-dimensional stratigraphy, the fundamental resonant frequency is given by

$$f = \frac{\overline{V_s}}{4h} \qquad (3)$$

where $\overline{V_s}$ is the average shear-wave velocity in the sediment layer. The microtremor HVSR method does not provide directly the shear-wave velocity structure, but this can be derived by modelling the spectral ratio curve provided that a constraint (on h or V_s) is available from independent surveys. Without a constraint, infinite models can fit the same HVSR curve in the same way. Thus, by assuming a stratified, one-dimensional soil model for the wave field and for the medium, a theoretical HVSR curve can be fitted to the experimental one to infer a subsoil model (Castellaro and Mulargia, 2009a).

4.2 REFRACTION MICROTREMOR (REMI) METHOD

In recent years the refraction microtremor (ReMi) method (Louie, 2001) has gained in popularity because of its limited equipment and space requirements. The method uses ambient ground motion recorded by a standard seismic refraction system with vertical geophones placed in a linear array. The basis of the analysis is the transformation of the measured data from a space-time domain to a frequency-slowness (inverse velocity) domain. This transformation is performed through the application of a "slant-stack" or "p-τ transformation" (Thorson and Claerbout, 1985) followed by a Fourier transform applied in the τ direction. The result of the analysis is a plot of signal power as a function of the frequency and slowness. Because the power levels can vary significantly at different frequencies, the spectrum is normalized. Depending on the shear-wave velocity structure and on the source distribution the ReMi method makes it possible to discriminate between various surface-wave modes (Beaty and Schmitt, 2003).

The use of linear geophone arrays means that an interpretation of the obtained images is not straightforward. In order to mitigate the problem of the apparent velocity, which comes from the fact that the direction of the propagation of waves in a passive survey is not necessarily parallel to the array, the general practise is to pick the dispersion curve not along the energy maxima in the phase-velocity spectra but somewhat below them (Louie, 2001). This procedure in the ReMi method implies a certain degree of subjectivity for determining the dispersion curve.

4.3 EXTENDED SPATIAL AUTOCORRELATION (ESAC) METHOD

The extended spatial autocorrelation (ESAC) method originates in the spatial autocorrelation (SPAC) method, which is based on research undertaken by Aki toward the end of the 1950s. The SPAC method's theoretical foundation is based on the precondition of a stochastic wavefield, which is stationary both in time and space (Aki, 1957). For the vertical component microtremor records from sensors deployed on a circumference with radius r and on its centre, azimuthal average of the autocorrelation coefficient, simply termed spatial autocorrelation coefficient ρ *(f, r)*, could be defined. In determining the phase velocity *c(f)* using the SPAC method, a fixed value of *r* is used. Then the spatial autocorrelation coefficient at the frequency *f* is related to the phase velocity of the Rayleigh waves *c(f)* via the Bessel function of the first kind of zero order $J_0(\ )$:

$$\rho(f,r) = J_0\left(\frac{2\pi f r}{c(f)}\right) \qquad (4)$$

The ESAC method is derived from the SPAC method by using a fixed value of *f* instead of a fixed value of *r* (Ohori et al., 2002; Okada, 2003). The spatial autocorrelation coefficient is fitted at each frequency *f* to a Bessel function $J_0(\ )$, which depends on the inter-station distances r_{0n} (the distances between the base station and the *n*-th station) as follows:

$$\rho_{0n}(f,r_{0n}) = J_0\left(\frac{2\pi f r_{0n}}{c(f)}\right) \quad n = 1,2,3...,N \qquad (5)$$

In this equation the only unknown is the phase velocity *c(f)*, which can be obtained from the inversion of the autocorrelation coefficients.

Two assumptions are made for those methods. Firstly, the Rayleigh wave microtremors are dominated by the fundamental mode and, secondly, the subsoil structure

under the array of observation is parallel. These methods cannot discriminate between the different modes (fundamental and higher) but will only show the predominant one (Okada, 2003). The SPAC method requires a circular array for data collection, but in urban areas it is difficult to deploy a circular array. The benefit of the ESAC method is that it does not require a circular array and is applicable to arbitrary arrays (L-shape, T-shape, cross-shape). A significant advantage of the SPAC and ESAC methods over the ReMi method is the extraction of the scalar wave velocity irrespective of the direction to the source and an omni-directional wave field (that is typical for urban areas) leads to better estimates of the scalar velocity (Asten, 2001). The identification of the dispersion curve in the SPAC and ESAC methods is not performed by picking the phase velocity and thus the results are not exposed to a subjective choice.

5 DATA ACQUISITION AND ANALYSES

Microtremor array surveys pose practical challenges in urban areas as very little open space is available for setting up the arrays. Thus the proper locations within the city were selected on the basis of aerial orthophoto images and field observations. The study area is limited by the Ljubljana highway ring and has an area of about 55 km^2. The selected locations correspond to city parks, school playgrounds and agricultural areas. The microtremor records were acquired at thirty such sites (Figure 12).

The microtremor array surveys were conducted by using a SoilSpy Rosina (Micromed) multichannel seismic digital acquisition system that offers a good signal-to-noise ratio (Micromed, 2008a). Twenty-four 4.5-Hz vertical geophones were planted to form a 2D array. For the ESAC analysis we used L-shape arrays and for the ReMi analysis the longer linear legs of the same arrays (Figure 4). Our task was to image the shear-wave velocity of the subsurface layers down to at least 30 m. Therefore, the frequency content of the records had to be low enough to obtain the phase velocities at large wavelengths as well. The geophone geometry was chosen according to the local situation. The corresponding dimensions of the arrays were between 42 and 75 m in length, with regular and irregular geophone inter-station distances (varying from 1 to 5 m), depending upon the available space. This information is summarized in Table 2 for all the 30 sites. The ambient noise was sampled during the day time for approximately 15 min at a 512-Hz sampling rate. We avoided performing measurements on artificial soil (e.g., asphalt, concrete and pavement), while stiff artificial soils may severely affect the HVSR curves (Castellaro and Mulargia, 2009b). The ReMi analysis was then performed using Soil Spy Rosina and Grilla software (Micromed, 2006; Micromed, 2008b). For both the ReMi and ESAC method the record was divided into 10-second, non-overlapping time windows and dispersion curves for each were computed. In the case of the ReMi non-informative time windows were removed and the final dispersion curve is the average of each time window dispersion curves. No time windows were removed in the case of the ESAC method and the final dispersion curve is also

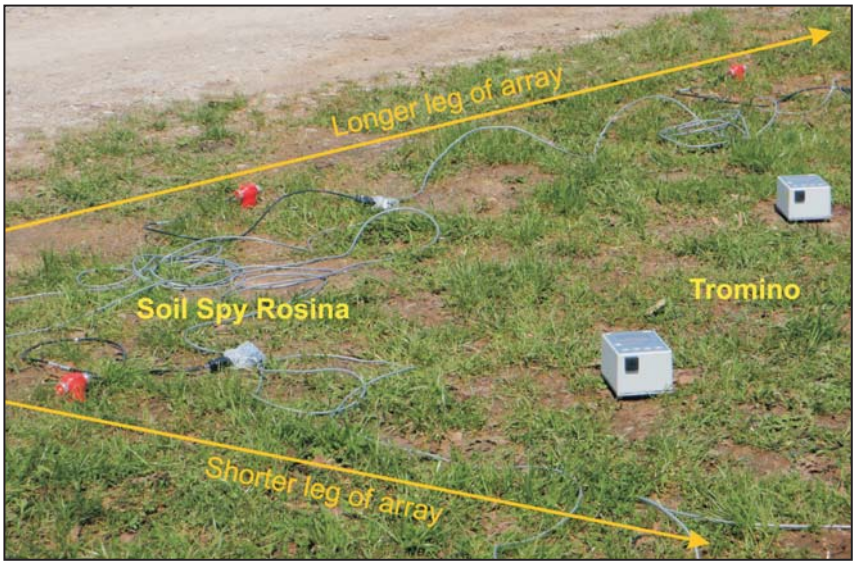

Figure 4. Part of L-shape microtremor array and the equipment used

Table 2. Data-acquisition parameters, fundamental soil frequency f_0 and *Vs30* results

Point	Coordinate X	Coordinate Y	Array L-shape geometry *	Geophone inter-station distance [m]	HVSR f_0 [Hz]	σ_{f_0}	*Vs30* ** [m/s]
SS 01	458976	99345	16 + 8	varying from 1 to 5	2.7	0.08	285
SS 02	460625	98439	16 + 8	3	1.2	0.01	225
SS 03	463246	97829	16 + 8	3	1.1	0.13	137
SS 04	461607	100062	16 + 8	3	2.3	0.08	266
SS 05	461943	101264	16 + 8	3	3.5	0.07	396
SS 06	463986	102671	16 + 8	3	2.6	0.11	530
SS 07	457571	101120	16 + 8	varying from 1 to 5	3.7	0.01	347
SS 08	458979	102780	16 + 8	varying from 1 to 5	2.9	0.05	357
SS 09	459227	103263	16 + 8	3	3.2	0.08	350
SS 10	459413	102716	16 + 8	varying from 1 to 5	3.7	0.02	339
SS 11	460528	99546	16 + 8	3	2.3	0.01	256
SS 12	464198	103737	16 + 8	5	2.3	0.06	557
SS 13	462971	103350	16 + 8	3	2.2	0.05	561
SS 14	465082	97149	16 + 8	3	2.1	0.02	235
SS 15	464495	98035	16 + 8	3	3.7	0.03	224
SS 16	462369	98766	16 + 8	3	2.2	0.10	149
SS 17	459481	100711	16 + 8	3	3.1	0.04	302
SS 18	460723	100853	16 + 8	3	3.8	0.07	232
SS 19	463018	100758	17 + 7	varying from 2 to 3	3.6	0.01	332
SS 20	463185	101590	14 + 5	varying from 2 to 3	2.5	0.26	585
SS 21	462576	102243	18 + 6	varying from 2 to 3	2.6	0.09	595
SS 22	460860	103347	17 + 7	3	2.1	0.16	515
SS 23	461579	104405	18 + 6	3	2.1	0.03	605
SS 24	465818	102771	18 + 6	3	3.1	0.06	545
SS 25	467418	102529	18 + 6	3	3.8	0.13	549
SS 26	466896	101553	18 + 6	3	3.3	0.05	465
SS 27	465641	101549	18 + 6	3	2.9	0.15	432
SS 28	465969	99974	18 + 6	3	4.4	0.16	393
SS 29	467257	100051	18 + 6	3	3.3	0.11	456
SS 30	458712	101060	16 + 8	3	2.7	0.01	336

* The number of geophones in the longer and in the shorter leg of the L-shaped array
** Typical uncertainty in Vs30 determination is of about 10-20% (Mulargia and Castellaro, 2009)

obtained as an average of all the time-window dispersion curves. An iterative grid-search procedure was used in both methods in order to find the values of the phase velocity that gives the best fit to the data.

During the deployment of the seismic array, single-station ambient microtremor noise was recorded as well at three or four locations along the array for 15 minutes at a 128-Hz sampling rate with a three-component, high-sensitivity Tromino tromograph (Micromed, 2005) developed for high-resolution digital measurements of the seismic noise. The data analysis to obtain the HVSR was performed using Grilla software (Micromed, 2006). The recorded noise was divided into 45 non-overlapping time windows, each being 20 seconds long. The signal of each window was corrected for the base line, padded

with zeroes and tapered with a Bartlett window. The relevant spectrogram was smoothed through a triangular window with a frequency-dependent half-width of 5% of the central frequency. For each time window both horizontal spectra (NS and EW direction) were geometrically averaged and then divided by the vertical spectra (Equation 2) to compute the HVSR curve. When transient signals were observed, the relevant portions of the recordings were rejected. This procedure influences only the reliability of the confidence interval and does not bias the average HVSR (D'Amico et al., 2004). The final HVSR curve with the relevant 95% confidence interval is obtained by averaging all the time-window HVSR curves.

The underground shear-wave velocity structure was obtained through joint modelling of the dispersion curve and the HVSR curve by using the Phase Velocity Spectra Module in the Grilla software (Micromed, 2008b and Micromed, 2007) that assumes a vertically heterogeneous, one-dimensional elastic model. This assumption was verified by taking several HVSR recordings along the array and comparing them. Some examples are shown in Figure 5, i.e., measurements along SS-02 (panel a), SS-16 (panel b), SS-19 (panel c) and SS-24 (panel d). All four cases show essentially identical HVSR curves and thus the assumption of 1D appears to be very well satisfied. The only difference is observed in the case of SS-24 in the frequency range 15 to 40 Hz (Figure 5 (d)), which corresponds to a depth of 3 to 5 m. We estimate that this difference is of minor importance.

The visual comparison between the ReMi and ESAC final dispersion curves was made to check their coherency. Finally, an interactive modelling of the final dispersion curve and the HVSR curve with a trial-and-error procedure to obtain a shear-wave velocity versus depth profile was performed. Each layer in a one-dimensional ground model is defined by its thickness (h), shear-wave velocity (V_s), longitudinal wave velocity (V_p) and mass densities (γ). It should be noted that V_p and the density ρ are of minor importance in determining the shape of the dispersion curve. The density ρ values have relatively small variations with depth, ranging from 1.6 to $2.1 \cdot 10^3$ kg/m^3. Moreover, the V_p value depends on V_s through the Poisson modulus ν (Equation 6), which was fixed to 0.35 during the process of modelling. In the case of this study the constraint is provided by the V_s of the first layer, inferred from the ReMi and ESAC methods applied at the same site.

$$\frac{V_s}{V_p} = \sqrt{\frac{0.5-\nu}{1-\nu}} \qquad (6)$$

In the starting models we introduced, at first, a solution of a maximum four layers. Then we estimate the thicknesses and velocities for the top two layers according to the HVSR and dispersion curves, fixing those values and then modelling the deeper layers. Once we had a satisfactory fit with the HVSR curve and the dispersion curves, we fixed the geometry of the layers and varied the layer velocities to estimate the best fit. During the modelling we fitted a synthetic model, not only to the main resonance frequency of the HVSR curve, which is in general the largest peak, but also to other stable humps and troughs in the HVSR curve.

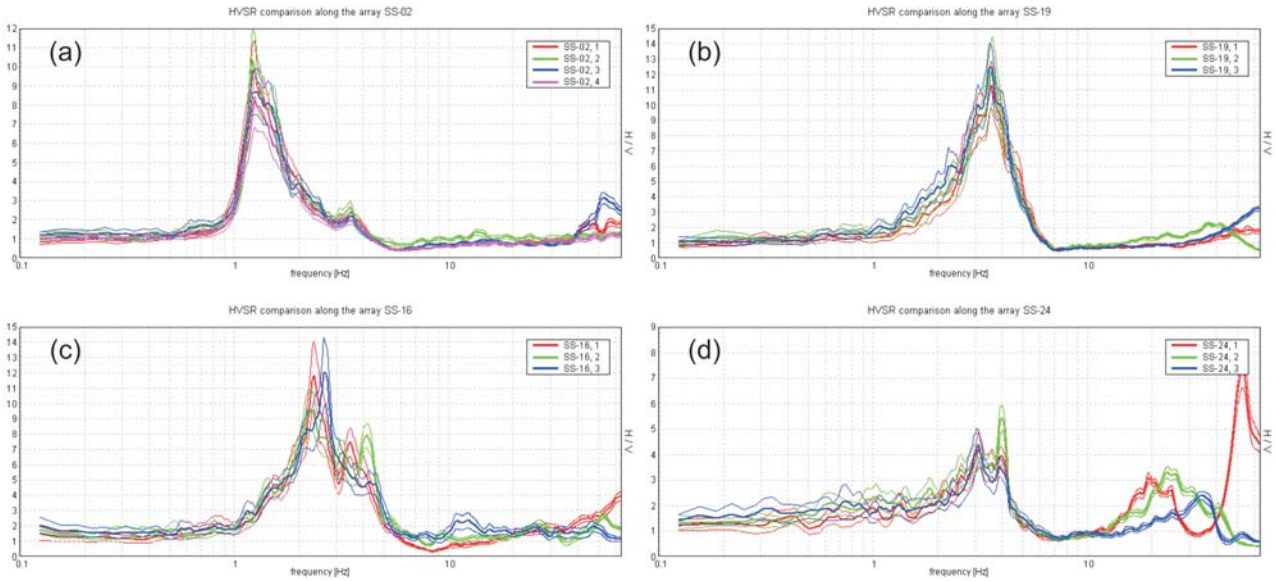

Figure 5. Comparison of the HVSR curve recorded at different places along the array; thicker lines are the average HVSR and the thinner lines represent the 95% confidence interval

Finally, the average shear wave velocity values in the upper 30 m (*Vs30*) were calculated in accordance with the following expression (CEN, 2004):

$$V_{s30} = \frac{30}{\sum_{i=1,N} \frac{h_i}{V_i}} \qquad (7)$$

where h_i and V_i denote the thickness (in metres) and the shear-wave velocity (at a shear strain level of 10^{-5} or less) of the *i*-th layer, in a total of *N*, existing in the top 30 m. In the end the *Vs30* data were used for the preparation of the shear-wave velocity distribution map of the study area in the topmost 30 m of sediments.

6 RESULTS AND DISCUSSION

The results of the microtremor measurements carried out in Ljubljana city include the HVSR curves, the Rayleigh wave-dispersion curves and the corresponding shear-wave velocity profiles. In Table 2 are the fundamental resonant soil frequency and *Vs30* values computed for each site. Some characteristic examples are shown in Figures 6 to 11; panel (a) shows the experimental HVSR curves (in a red colour, the black lines present the 95% confidence interval) and the fitted synthetic HVSR curves in the blue coloured solid line. The comparison between the experimental dispersion curves from the ReMi and ESAC methods with the theoretical one is shown in panel (b). The dispersion curves derived from the ESAC are shown with yellow circles and the ReMi dispersion curves are shown as contour plots. The light blue circles indicate the theoretical Rayleigh wave phase dispersion curves obtained by joint modelling and corresponding to the shear-wave velocity profile shown in panel (c).

The main purpose of the HVSR measurements was not to estimate the soil's fundamental frequency of resonance but to operate a joint fit of the HVSR and dispersion curves and to verify the 1D soil assumption underlying array techniques. However, the values are in good agreement with results from Gosar et al. (2010). Clear peaks were obtained in the whole southern part of the city (i.e., Figures 3 and 9) and also at some sites in the northern part (i.e., Figure 8). Generally, the northern part of the city is characterized by HVSR curves showing two or more peaks with modest amplitude (Figures 7, 10, and 11), denoting subsoil locally characterized by two or more significant impedance contrasts at different depths. A second peak occurs at frequencies above 10 Hz, suggesting a very shallow seismic interface. This ascertainment corresponds to known information about the complex geology of stiffer cemented gravel horizons inside the sedimentary cover in this area.

For most sites, the velocity of the Rayleigh dispersion increases continuously as the frequency decreases, indicating a continuously increasing shear-wave velocity with depth. The phase velocity estimates from the ReMi and ESAC methods are very consistent in the high-frequency range, i.e., from 15 to 35 Hz. In the frequency range below 5 Hz both methods were less effective due to the limited geometry of field lay-out and the limitations of the 4.5-Hz geophones. Furthermore, the depth penetration of an array is more often limited by the presence of strong impedance contrast at some depth rather than by the array geometry. In the case of the presence of a strong impedance contrast the most part of waves would be reflected and keep travelling in the shallow layer only, and thus not provide any information about the structure below that shallow layer. Usually, in the absence of strong impedance contrast it is feasible to inspect depths of 4 times the array length. The results from the ReMi method were severely limited below 10 Hz where the dispersion curves become less coherent, but generally allowed good coverage of the phase velocity in the high-frequency range up to 50 Hz (evident from Figures 6 to 10), except in the case SS-27 (Figure 11). The low-frequency limit of the dispersion curve from the ESAC is in agreement with that from the HVSR curve, as at the resonant frequency the vertical component of the Rayleigh wave vanishes and therefore the phase-velocity values are reliable only from that frequency onwards (Scherbaum et al., 2003). On the other hand, in some cases the ESAC method was unable to provide clear information above 20 Hz (e.g., SS-11, SS-12 and SS-27). From the ReMi contour plot for site SS-03 the fundamental mode of the dispersion curve, as well as two higher modes, is observed (Figure 6). Only the fundamental mode is visible in the case of SS-06, SS-10 and SS-11 (Figures 7 to 9). The fundamental modes from the ReMi method and the resulting curves from the ESAC method, which only shows the predominant one, agree well. Hence it follows that in most cases the higher mode does not severely mask the fundamental mode in the ESAC curves. There were only a few exceptions, where the higher mode in a certain frequency range is dominant over the fundamental one. The Rayleigh dispersion result of the ESAC method at site SS-12 shows that the dispersion in the frequency range 20–40 Hz corresponds to a higher mode, which is evident from the comparison with the dispersion curves of the ReMi contour plot (Figure 10). Joint modelling with the HVSR data has proved very useful to constrain the model parameters and reduce the ambiguity, which cannot be avoided if only the dispersion curves are used to derive a velocity profile.

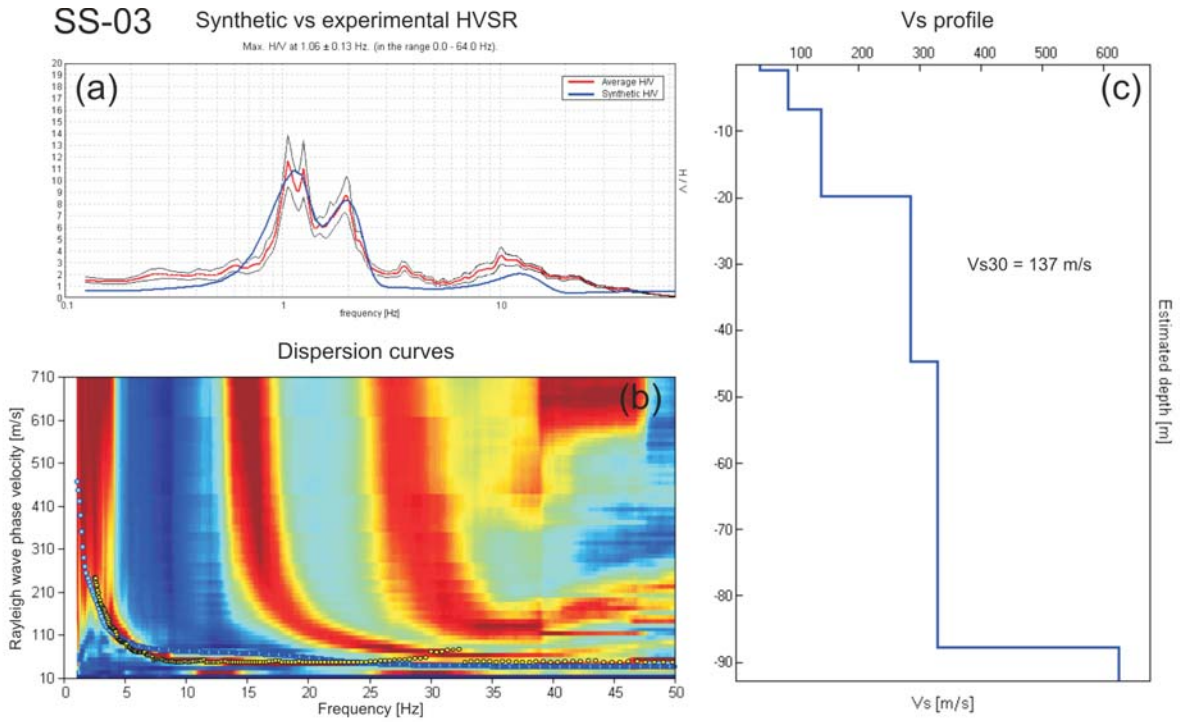

Figure 6. Site SS-03 (a) The experimental HVSR curve in red (black lines present the 95% confidence interval) and the fitted synthetic HVSR curve in blue (b) The comparison between experimental dispersion curves from the ReMi (contour plot) and ESAC (yellow circles) methods with the theoretical one (blue circles) (c) Corresponding shear-wave velocity profile

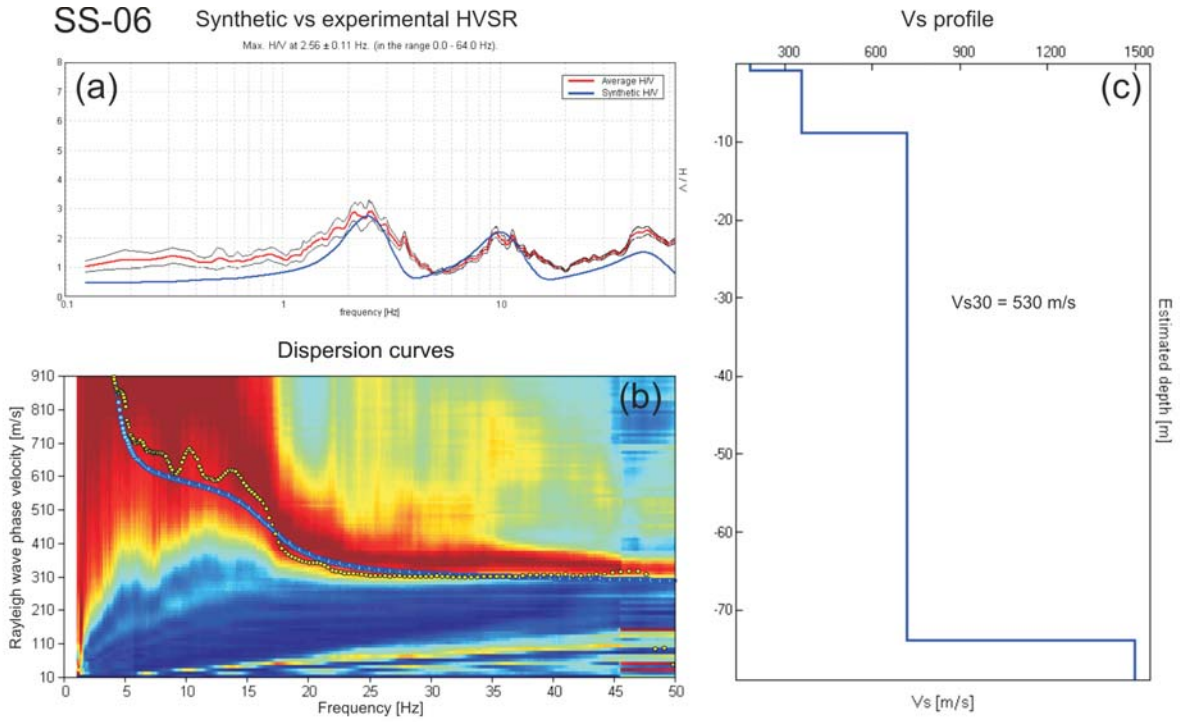

Figure 7. As in Figure 6, but for site SS-06

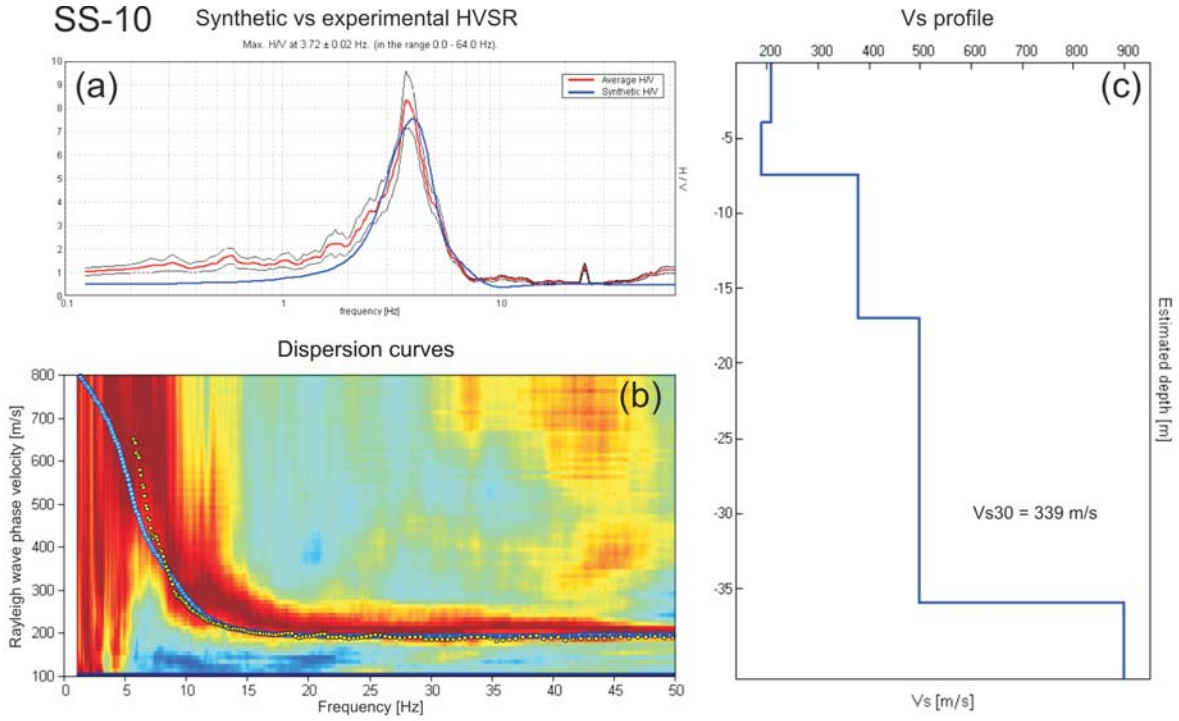

Figure 8. As in Figure 6, but for site SS-10

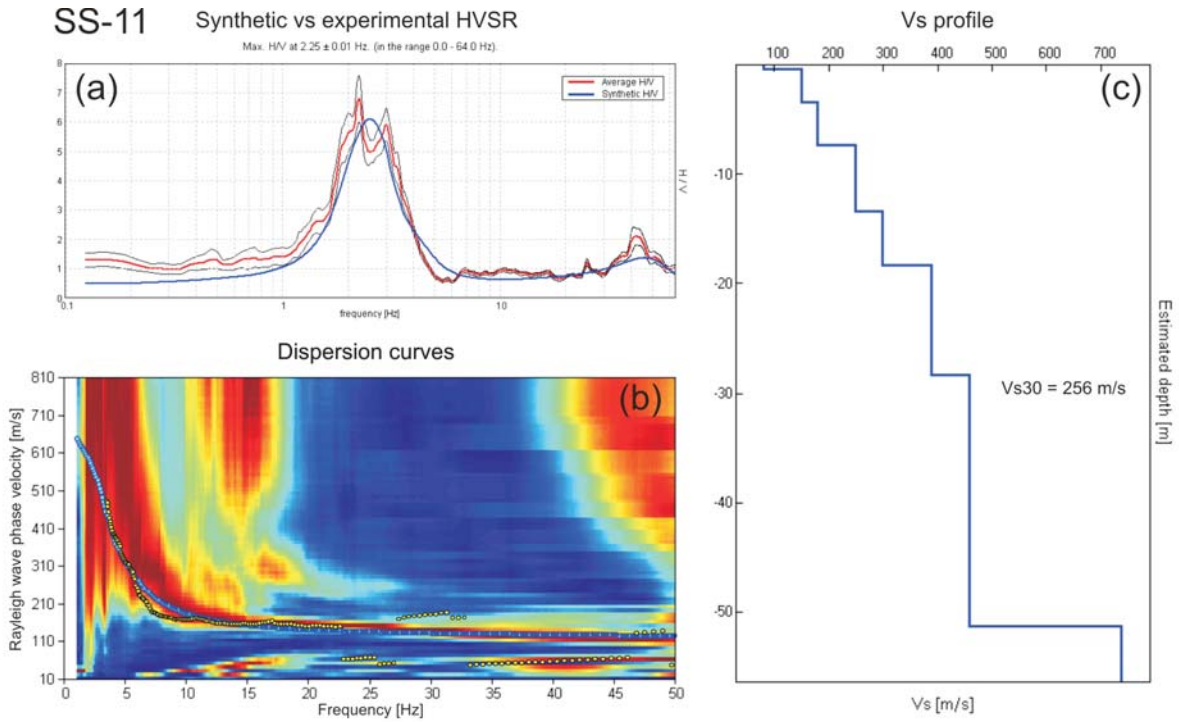

Figure 9. As in Figure 6, but for site SS-11

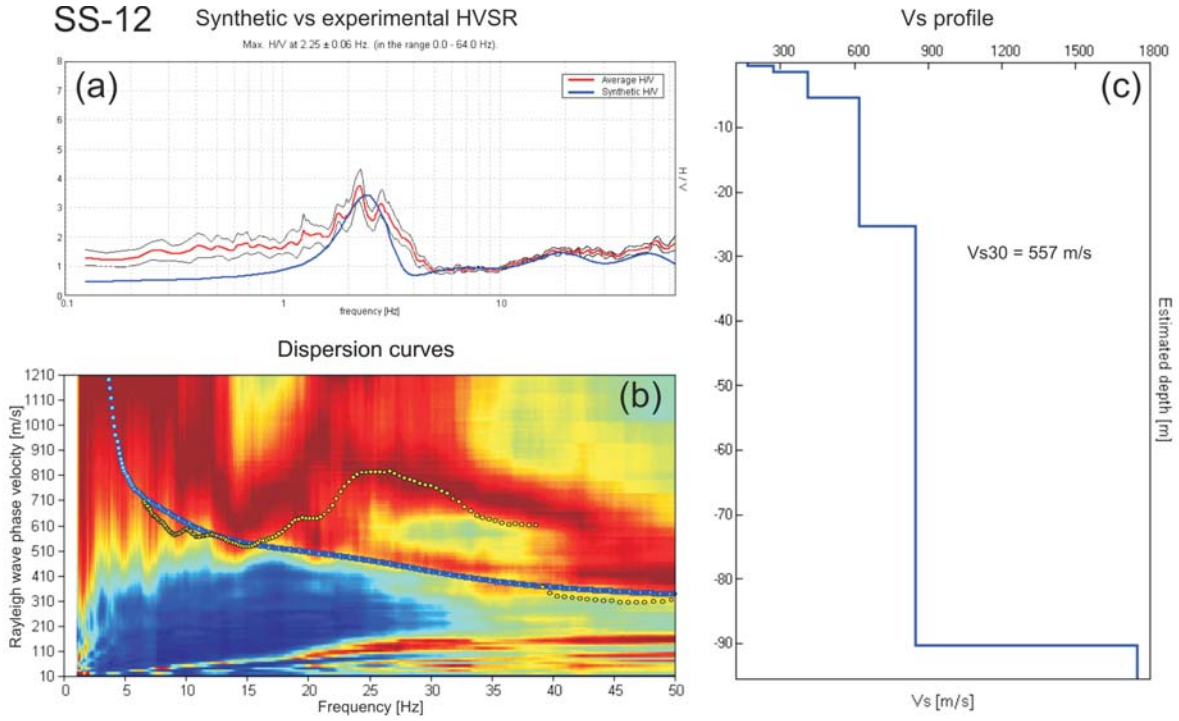

Figure 10. As in Figure 6, but for site SS-12

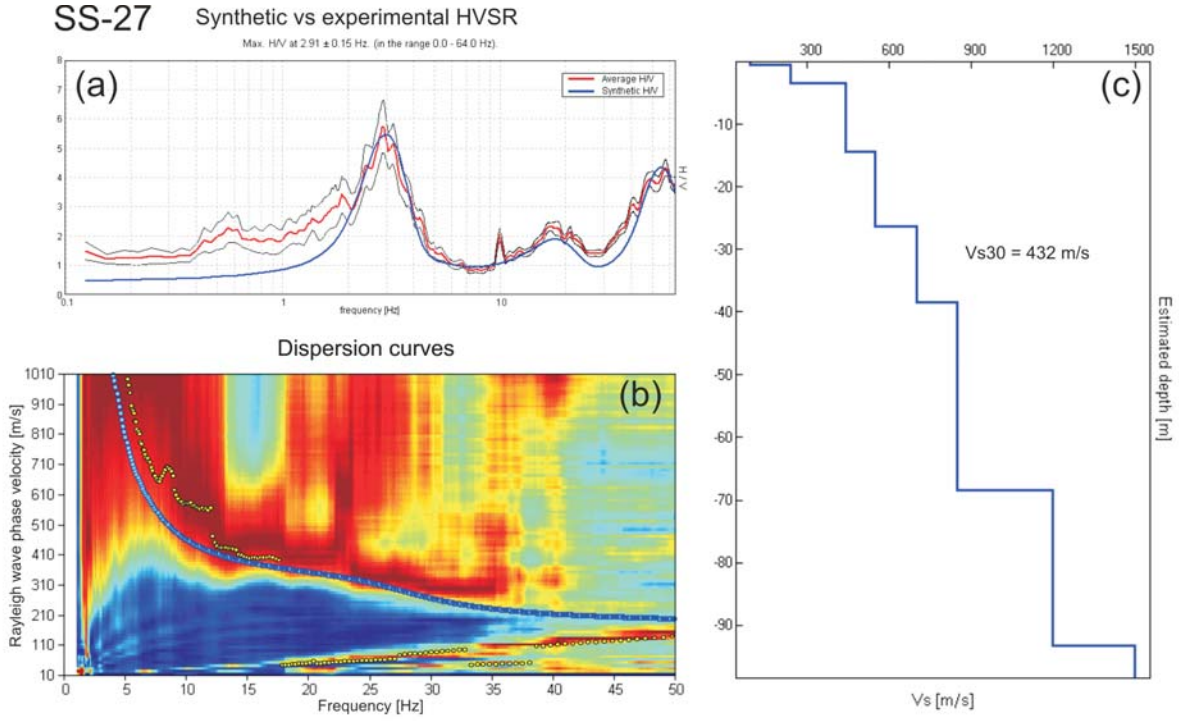

Figure 11. As in Figure 6, but for site SS-27

The calculated shear-wave velocity distribution down to a depth of 30 m in Ljubljana city is presented in Table 2 and in Figure 12. Black circles on the figure mark the location of the 30 measuring points. The *Vs30* distribution map is overlaid over the existing microzonation based on the EC8 (Zupančič et al., 2004). On the basis of *Vs30* values the study area can be classified as ground type B (360–800 m/s), C (180–360 m/s), D and E (< 180 m/s). The northern part of the study area, located in the Ljubljana Field, has higher shear-wave velocity values, within the range 360–600 m/s, and thus falls into the ground type B. The low-velocity sites are in general related to Ljubljana Moor and correspond to the ground types C, D and partly E. According to our study, the sites have been generally classified into higher soil classes, i.e., having better seismological and geotechnical properties than indicated by previous study.

A comparison of the geological map (Figure 2) and the *Vs30* map shows very good agreement, reflecting the fact that low velocities in the southern part correspond to soft lacustrine and fluvial Quaternary sediments. The *Vs30* values are then increasing towards the north, where stiffer material (Pleistocene and Holocene glaciofluvial deposits) is dominant. Also, a comparison with the sediment resonant frequency map (Figure 3) clearly highlights the relations between the fundamental soil frequency, the shear-wave velocity and the thickness (Equation 3) known from sparse geotechnical data.

7 CONCLUSIONS

Although no damaging earthquakes have occurred since 1963 in the vicinity of Ljubljana, this area is one of the most seismically active regions in Slovenia. For this reason, microzonation studies are very important for earthquake engineering design. The Eurocode 8, which constitutes the standard for seismic-resistant design in

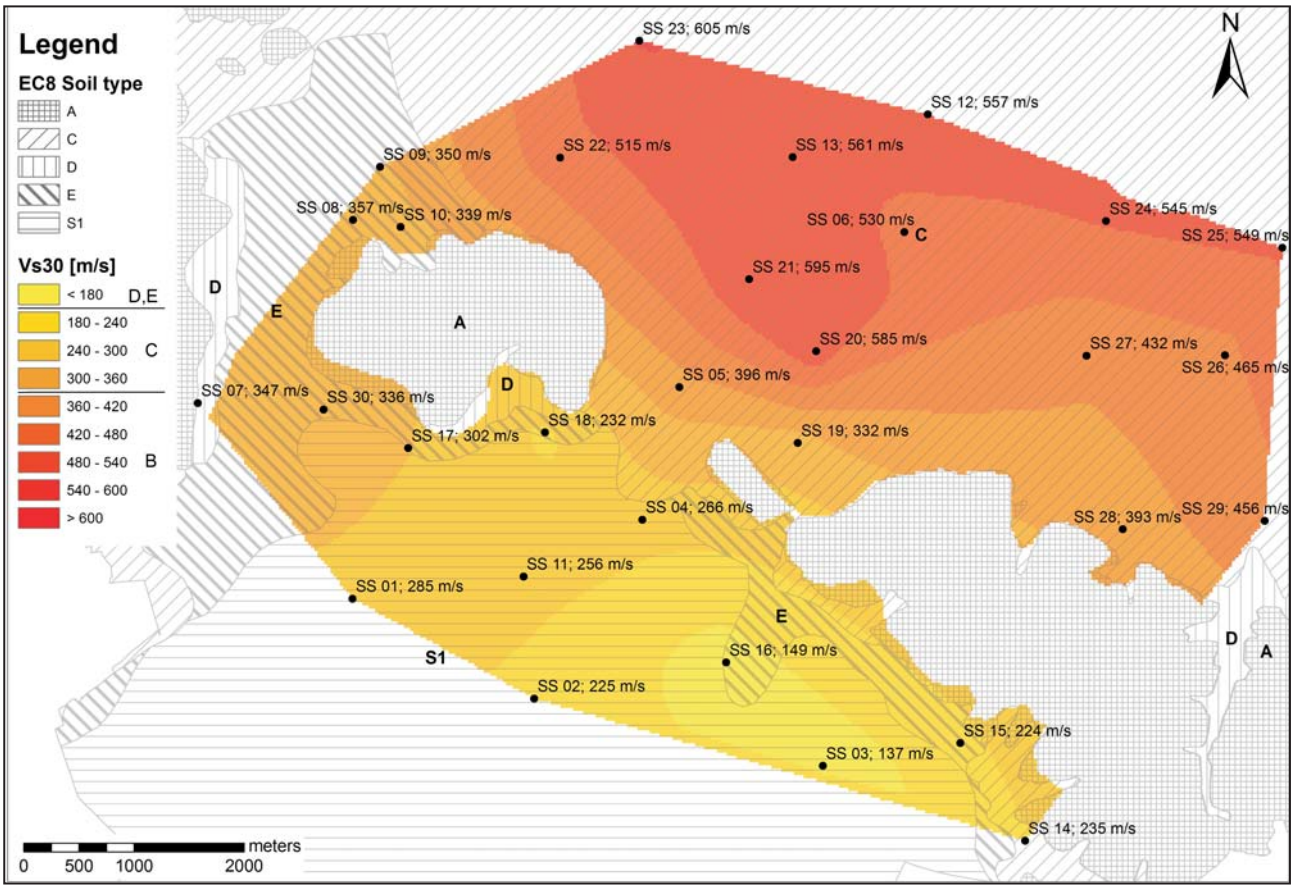

Figure 12. *Vs30* distribution map (coloured contour plot) and previous soil classification for Ljubljana (after Zupančič et al., 2004) according to EC8 ground types (b & w hatching plot)

Europe and also in Slovenia, adopts as a key quantitative parameter, the average shear-wave velocity in the first 30 m of subsoil, commonly termed as *Vs30*.

In this paper the results of the shear-wave velocity determination in the top 30 m (*Vs30*) based on joint modelling of the HVSR, ReMi and ESAC microtremor data are presented. The ReMi and ESAC methods provided very similar phase-velocity dispersion curves at all 30 measuring sites in Ljubljana city. The combination of both methods made it possible for the dispersion curves of the fundamental mode Rayleigh wave to be determined for the frequencies from approximately 2 Hz and up to 50 Hz. The dispersion curves were further used to develop one-dimensional, shear-wave velocity profiles from which the *Vs30* values were calculated. Simultaneous HVSR modelling has proved to be very useful to constrain model parameters and reduce ambiguity, which cannot be avoided if only dispersion curves are used to derive a velocity profile. Based on the *Vs30* values the study area can be classified as ground types B, C, D and E. In general, the study area could be divided into two parts with different average velocities. In the northern part, higher velocities were obtained, ranging from 360–600 m/s, and thus correspond to ground type B. Lower velocities are characteristic for the whole southern part of Ljubljana. The values there are below 300 m/s with the lowest shear-wave velocity of 137 m/s and the area is therefore classified as ground types C, D and E. The results suggest an interesting difference in comparison with the previous microzonation based on EC8 (Zupančič et al., 2004). The velocities obtained in this study indicate that soils have better seismogeological conditions and can be classified in general to one ground type class better according to EC8 that in the previous study. It should be stressed that the previous microzonation did not involve any direct shear-wave velocity measurements.

Although *Vs30* is perhaps not the most suitable parameter to define seismic site response, it is presently requested by many national seismic regulations. Nevertheless, the spatial distribution of *Vs30* has provided valuable information to integrate and supplement existing seismic microzonations of Ljubljana. The true progress of this study is the acquisition of several Vs profiles that are much more informative than *Vs30* alone and can be used for direct, one-dimensional modelling of the seismic ground motion.

ACKNOWLEDGMENTS

The authors are indebted to Tjaša Mlinar for her help with the field measurements. Thanks are due to Polona Zupančič for the compilation of the seismicity and geological map in Figures 1 and 2. The study was realized with the support of research program P1-0011 and grant 1000-05-310228 financed by the Slovenian Research Agency.

REFERENCES

Aki, K. (1957). Space and time spectra of stationary stochastic waves, with special reference to microtremors. Bulletin of the Earthquake Research Institute 35: 415-456.

Aki, K. and Richards, P.G. (2002). Quantitative Seismology, 2nd Edition. University Science Books, 700 pp.

Anderson, J.G. (2007). Physical Processes That Control Strong Ground Motion. In Hiroo Kanamori, Volume Editor; Gerald Schubert, Editor in Chief (Ed.), Treatise on Geophysics, Vol. 4, Earthquake Seismology (Vol. 4, 513-565). Amsterdam: Elsevier.

Asten, M.W. (2001). The spatial auto-correlation method for phase velocity of microseisms – another method for characterisation of sedimentary overburden: in Earthquake Codes in the Real World, Australian Earthquake Engineering Society, Proceedings of the 2001 Conference, Canberra.

Bard, P.Y. (1999). Microtremor measurements: a tool for site effect estimation? In: Irikura, K., Kudo, K., Okada, H., Sasatami, T. (Editors) The effects of surface geology on seismic motion. Balkema, Rotterdam, pp 1251-1279.

Beaty, K.S. and Schmitt, D.R. (2003). Repeatability of multimode Rayleigh-wave dispersion studies. Geophysics 68: 782-90.

Castellaro, S., Mulargia, F., Rossi, P.L. (2008). Vs30: Proxy for Seismic Amplification? Seismological Research Letters, Vol. 79, No. 4: 540-543.

Castellaro, S., Mulargia, F. (2009a). Vs30 estimates using constrained H/V measurements. Bulletin of the Seismological Society of America 99: 761-773.

Castellaro, S., Mulargia, F. (2009b). The effect of velocity inversions on H/V. Pure and Applied Geophysics 166: 567-592.

CEN (2004). Eurocode 8—design of structures for earthquake resistance. Part 1: general rules, seismic actions and rules for buildings. European standard EN 1998-1, December 2004, European Committee for Standardization, Brussels

D'Amico, V., Picozzi, M., Albarello, D., Naso, G., Tropenscovino, S. (2004). Quick estimates of soft sediment thicknesses from ambient noise horizontal to vertical spectral ratios: a case study in southern Italy. Journal of Earthquake Engineering 8: 895-908.

Gosar, A., Rošer, J., Šket-Motnikar, B., Zupančič, P. (2010). Microtremor study of site effects and soil-structure resonance in the city of Ljubljana (central Slovenia). Bulletin of Earthquake Engineering 8: 571-592.

Grad, K. and Ferjančič, L. (1974). Basic geological map of Yugoslavia 1:100.000 – sheet Kranj. Geological Survey of Slovenia, Ljubljana.

Lapajne, J. (1970). Seismic microzonation of Ljubljana – geophysical investigations. Geological Survey of Slovenia, Ljubljana, 16 pp.

Lapajne, J., Šket-Motnikar, B., Zupančič, P. (2001). Design ground acceleration map of Slovenia. Potresi v letu 1999: 40-49.

Louie, J. (2001). Faster, better: shear-wave velocity to 100 meters depth from refraction microtremor arrays. Bulletin of the Seismological Society of America 91: 347-364.

Medvedev, S.V. (1965). Inženjerska seizmologija. Gradjevinska knjiga, Belgrade, 271 pp.

Mencej, Z. (1989). The gravel fill beneath the lacustrine sediments of the Ljubljansko barje. Geologija 31-32: 517-553.

Micromed (2005). Tromino, portable seismic noise acquisition system, user's manual. Micromed, Treviso, 101 pp.

Micromed (2006). Grilla ver. 2.2, spectral and HVSR analysis – user's manual. Micromed, Treviso, 47 pp.

Micromed (2007). An introduction to the H/V inversion for stratigraphic purposes. Micromed, Treviso, 31 pp.

Micromed (2008a). SoilSpy Rosina ver. 2.0 – user's manual. Micromed, Treviso, 81 pp.

Micromed (2008b). An introduction to the phase velocity spectra module in Grilla. Micromed, Treviso, 16 pp.

Mucciarelli, M. and Gallipoli, M.R. (2001). A critical review of 10 years of microtremor HVSR technique. Bolletino di Geofisica teorica ed applicata 42: 255-266.

Mulargia, F. and Castellaro, S. (2009). Experimental Uncertainty on the Vs(z) Profile and Seismic Soil Classification. Seismological Research Letters, Vol. 80, No. 6: 985-988.

Nakamura, Y. (1989). A method for dynamic characteristics estimation of subsurface using microtremor on the ground surface. Quarterly Report of Railway Technical Research Institute (RTRI) 30: 25-33.

Nakamura, Y. (2000). Clear identification of fundamental idea of Nakamura's technique and its applications. 12WCEE, Auckland.

Nogoshi, M. and Igarashi, T. (1970). On the propagation characteristics estimations of subsurface using microtremors on the ground surface. Jour. Seismol. Soc. Japan 23, 264-280.

Nogoshi, M. and Igarashi, T. (1971). On the amplitude characteristics of microtremor (Part 2) (in Japanese with English abstract). Jour. Seism. Japan 24, 26-40.

Ohori, M., Nobata, A., Wakamatsu, K. (2002). A comparison of ESAC and FK methods of estimating phase velocity using arbitrarily shaped microtremor arrays. Bulletin of the Seismological Society of America 92, 2323-2332.

Okada, H. (2003). The microtremor survey method. American Geophysical Monograph 12, Society of Exploration Geophysicist, 135 pp.

Premru, U. (1982). Basic geological map of Yugoslavia 1:100.000 – sheet Ljubljana. Geological Survey of Slovenia, Ljubljana.

Scherbaum, F., Hinzen, K.G., Ohrnberger, M. (2003). Determination of shallow shear wave velocity profiles in Cologne Germany area using ambient vibrations. Geophysical Journal International 152: 597-612.

SIST EN 1998-1:2005/oA101 (2005). Eurocode 8, design of structures for earthquake resistance – part 1: general rules, seismic actions and rules for buildings, national Annex. Slovenian institute for standardization, Ljubljana.

Thorson, J.R. and Claerbout, J.F. (1985). Velocity-stack and slant-stack stochastic inversion. Geophysics 50: 2727-41.

Žlebnik, L. (1971). Pleistocen Kranjskega, Sorškega in Ljubljanskega polja (Pleistocene of Kranj, Sora and Ljubljana Field). Geologija 14, 5-52.

Zupančič, P., Šket-Motnikar, B., Gosar, A., Prosen, T. (2004). Seismic microzonation map of the municipality of Ljubljana. Potresi v letu 2002: 32-54.